European Polymer Journal 47 (2011) 584–599

Contents lists available at ScienceDirect

European Polymer Journal

journal homepage: www.elsevier.com/locate/europolj

Feature Article - Macromolecular Nanotechnology

Supramolecular assemblies of block copolymers as templates for fabrication of nanomaterials

Bhanu Nandan *, Biplab K. Kuila, Manfred Stamm *

Leibniz Institute of Polymer Research Dresden, Hohe Strasse 6, 01069 Dresden, Germany

ARTICLE INFO

Article history:
Available online 23 October 2010

Dedicated to Professor Nikos Hadjichristidis in recognition of his contribution to polymer science.

Keywords:
Block copolymer
Supramolecular assemblies
Nanotemplate
Nanomaterials
Self-assembly
Thin films

ABSTRACT

Self-assembled polymeric systems have played an important role as templates for nanofabrication; they offer nanotemplates with different morphologies and tunable sizes, are easily removed after reactions, and could be further modified with different functional groups to enhance the interactions. Among the various self-assembled polymeric systems, block copolymer supramolecular assemblies have received considerable attention because of the inherent processing advantages. These supramolecular assemblies are formed by the non-covalent interactions of one of the blocks of the block copolymer with a low molar-mass additive. Selective extraction of the additive leads to porous membranes or nano-objects which could then be used as templates for nanofabrication leading to a variety of ordered organic/inorganic nanostructures. In this feature article, we present an over-view of the recent developments in this area with a special focus on some examples from our group.

1. Introduction

The rapid growth of nanoscience and nanotechnology has pushed the scale limits of modern functional devices that demand materials at the nanometer scale. Controlling the structure of these material at the nanometer scale and assembling these nanomaterials into arrays and networks in a controlled manner are the keys to new technologies. The fabrication of arrays of nanomaterials, however, with nanoscale precision remains a formidable task. Selective positioning of nanomaterials is always challenging, and special techniques are often needed to achieve this goal. The traditional methods used to fabricate such periodic arrays employs the top-down approaches like e-beam lithography [1], nanoimprinting [2], focused-ion-beam lithography [3]. The problem here is that direct writing is a serial process and structuring of large areas takes very long time and is very expensive [1–3]. Another important aspect, a feature size less than 30 nm is hard to achieve with the above-mentioned standard semiconductor lithography techniques.

An alternative route to nanostructures and arrays is the so-called "bottom-up" approach utilizing self-assembly of organic and inorganic material at surfaces which can offer advantages including experimental simplicity, the possibility of three-dimensional assembly and the potential for low-cost mass fabrication. Block copolymers are known to self-assemble at molecular scale into variety of nanoscale structures such as lamellar, cylindrical, or spherical nanodomains (among other more complex morphologies) with dimensions from a few nanometres to above 100 nm [4,5] depending on molecular weight, segment size, and the strength of interaction between the blocks, represented by the Flory–Huggins interaction parameter, χ. Significant progress has been achieved in controlling the orientation and

* Corresponding authors. Present address: Department of Textile Technology, Indian Institute of Technology – Delhi, New Delhi, India. Tel.: +49 3514658 224; fax: +49 3514658 281.

E-mail addresses: bhanunandan@hotmail.com (B. Nandan), stamm@ipfdd.de (M. Stamm).

0014-3057 © 2010 Elsevier Ltd. Open access under CC BY-NC-ND license.
doi:10.1016/j.eurpolymj.2010.09.033

long-range ordering of the block copolymer microdomains both in bulk as well as in thin film. Moreover, the separation and orientation of the domains are also influenced, especially in thin films, by surface–interfacial interactions, kinetic aspects during preparation (non-equilibrium structures) as well as by the interplay between structural periodicity and film thickness. These self assembled nanostructures are promising [6–12] for fabrication of metal, magnetic, polymeric, semiconducting nanomaterial different shapes as sphere, rods and tubes or their large scale ordered arrays of high density (terabits per cm^2) used for electronic, electrochemical, optoelectronic, magnetic, photonic, and biosensing device applications.

In recent years, it was demonstrated that a supramolecular approach to block copolymer self-assembly is a simple and powerful technique for fine tuning of the block copolymer morphologies, and has been successfully applied in bulk [13–16] and in thin films [17–21]. Block copolymer supramolecular assembly (SMA) where a low molar-mass additive molecule is attach to the side chains of one of the block of the block copolymer by different non-covalent interactions [15–27], also microphase separate similar to block copolymer into arrays of microdomains, tens of nanometers in size [17,19]. These supramolecules offer advantages over the covalently linked analogues, since different functionalities can be introduced into the assemblies simply by substituting the small molecules, there by avoiding the need to synthesize entirely new families of BCP based supramolecules [28,29].

A number of tunable morphologies are readily accessible using a single BCP either by varying the stoichiometry between the small molecules and BCPs or by redistributing the small molecules between the two microdomains using external stimulus, like heat [13], electric field [29]. Another major advantage of SMA strategy is that the low molar-mass additive can be removed easily from the SMA by selective dissolution to obtain a nanoporous material [17,19]. These nanopores and nanochannels are lined with functional groups that are readily available for further functionalization. The pioneering work on such materials was done in the groups of Olli Ikkala and Gerrit ten Brinke [15,30,31]. They demonstrated that such materials may also exhibit hierarchical structures displaying structure-within-structure pattern characterized by two length scales.

Our group in past few years have also worked extensively on block copolymer SMAs mostly with an aim to fabricate polymer nanotemplates for further nanofabrication. One of the systems widely studied by us consists of SMAs formed by poly(styrene)-*b*-poly(4-vinylpyridine) (PS-*b*-P4VP) and 2-(4′-hydroxybenzeneazo) benzoic acid (HABA) where P4VP(HABA) comb block forms cylindrical microdomains surrounded by PS matrix [17]. This supramolecular system shows the reversible switching of the orientation of the microdoamin (for example: parallel cylinder to perpendicular cylinder) upon exposure to solvent vapours. Selective extraction of HABA creates pores or polymeric nano-objects which we used as templates for nanofabrication. In this feature article we focus on the progress made in our group on such materials and the various approaches adopted for utilizing the polymeric nanotemplates for the nanofabrication.

2. Synthesis of block copolymer supramolecular assemblies

For preparation of block copolymer supramolecular assemblies, at least one of the blocks of the block copolymer should contain suitable functionality which can interact with the low-molecular weight additive through non-covalent interactions. The most commonly used block copolymers for such an approach are polystyrene-block-poly(4-vinylpyridine) (PS-*b*-P4VP) and polystyrene-block-poly(ethylene oxide) (PS-*b*-PEO). The low-molecular weight additives which have been extensively used are 3-pentadecylphenol (PDP), dodecylbenzene sulfonic acid (DBSA), and 2-(4′-hydroxybenzeneazo) benzoic acid (HABA). However, in general, a range of low-molecular weight additives with different functionality can be used as long as they contain suitable functionality to form supramolecular complexes with the block copolymer to form a comb like block copolymer. The typical synthesis of the supramolecular assemblies involves mixing of the block copolymer and low-molecular weight additive in desired ratio in a common solvent for several hours. Bulk samples are prepared by evaporating the solvent whereas thin films on desired substrates are prepared by spin or dip coating. A further solvent/thermal annealing step is necessary for the long-range ordering of the self-assembled structures.

If the low-molecular weight additive is sufficiently long, the block copolymer supramolecular assemblies show hierarchical self-assembly. In this case microphase separation occurs on two length scales, the larger length-scale structure formed by the polymer blocks and the smaller length-scale structure is formed by the comb block i.e. the polymer block containing the low-molecular weight additive. Such supramolecular comb-coil complexes have been drawing significant interest recently due to their potential use as functional materials in electrical, optical, and other functionalities [15,29,32]. The self-organized domains at multiple length scales offer switch-like controls of material functionalities by the relevant order–disorder or order–order transitions [15,30,33,34]. Ikkala and co-workers have extensively studied such supramolecular assemblies with hierarchical structures and have reported a range of morphologies: lamellar-within-spherical, lamellar-within-cylinder, lamellar-within-lamellar, cylinder-within-lamellar, and spherical-within-lamellar structures [13,14]. The morphology tuning can be done simply by varying the ratio of the block length and/or by changing the molar ratio between the monomeric unit of the functional block and the additive. The role of molecular architecture of the block copolymer on the microphase separation in such supramolecular assemblies have also been studied. Moreover, it has also been shown that some novel morphologies could be formed which generally are not observed for simple block copolymers. Chen et al. and Nandan et al. have shown the formation of square packed cylinders in the system they studied [35,36].

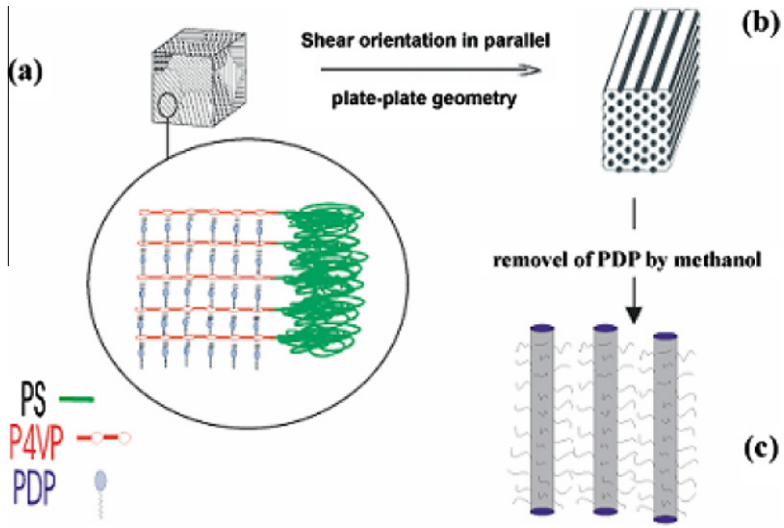

Fig. 1. Schematic illustration for fabrication of functional nano objects using block copolymer supramolecular assembly (a) bulk sample with microphase separated regions which are randomly ordered (b)macroscopically oriented sample after application of shear (c) individual cylinders composed from PS core and P4VP brushes after removal of PDP [37a].

3. Nanotemplates from block copolymer supramolecular assemblies

The significant interest recently attracted by the block copolymer supramolecular assemblies is largely due to the fact that the removal of the low-molecular weight additive from the bulk or thin film sample can readily generate polymeric nano-objects or nanoporous membranes. The removal of the low-molecular weight additive is possible if they are bound to the block chain by weaker interactions such as hydrogen bond. Moreover, since the walls of the polymeric nano-objects or membranes are lined with functional polymeric chains, they potentially could be used as templates for further nanofabrication.

Fig. 1 illustrates a typical approach for producing functional nano-objects from bulk samples of block copolymer supramolecular assemblies [31,37a]. A polystyrene-block-poly(4-vinylpyridine) (PS-*b*-P4VP) was mixed with a low-molecular weight additive, 3-pentdecylphenol (PDP). The bulk sample formed from solution showed hexagonally packed PS cylinders in a matrix formed by P4VP(PDP) comb blocks. The grain size of the hexagonally packed PS cylinders were rather small in the as-prepared sample. After applying shear, the long-range order of the cylinders could be significantly improved and, hence, infinitely long PS cylinders are also formed. In the next step the sample is immersed in a PDP selective solvent such as ethanol. The solvent washes out PDP from the supramolecular assembly leaving behind individual PS cylinders. The P4VP chains which are covalently bonded to PS blocks collapse on the wall of the PS cylinders. Fig. 2(a and b) shows representative AFM height images obtained on thin

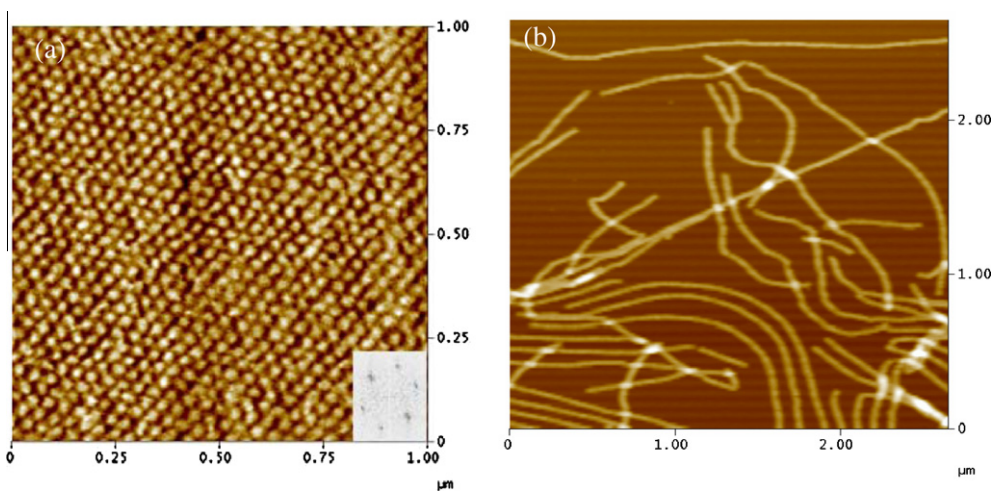

Fig. 2. AFM height image of PS-*b*-P4VP (PDP) block copolymer supramolecular assembly (a) thin section of the supramolecular assembly bulk sample (b) thin section of the supramolecular bulk sample after extraction of PDP [37a].

section of supramolecular assembly formed by PS-*b*-P4VP (21–20 k) with PDP before and after extraction of PDP. The AFM height image before PDP extraction shows hexagonally arranged PS cylinders in P4VP(PDP) matrix. After extracting the PDP, the structure collapses leaving behind isolated PS cylinders of nanometre diameters. These PS cylinders have wall covered with collapsed P4VP chains.

A different approach for producing long isolated polymeric nanofibres involved melt-spinning of PS-*b*-P4VP(PDP) supramolecular assemblies [38]. Fig. 3 shows the spinning device used for producing the SMA nanofibres. Spinning was done at 120 °C. The fibres broke up if the distance between the die and the winder was larger than 50 cm. The filament seemed to break under its own weight because of the low melt strength of the material. Consequently, the winder was rearranged at a distance of 20 cm below the die to avoid fibres break-up. The take-up velocity for winding was chosen in the same range as the extrusion velocity. The maximum possible draw ratio was not greater than two and the used take-up velocity had to be adjusted carefully. Therefore, the process was an extrusion process where only little elongational deformation was possible but still macroscopically oriented fibres were produced. The filaments, defined as oriented fibres after the melt spinning process, were inspected by light microscopy to study the large-scale alignment and macroscopic appearance. Fig. 4(a) shows a light microscopic image of the polymeric complex filament with a diameter of about 300 μm. Apparently, the production of filaments could be achieved with very smooth surfaces. Macroscopically oriented filaments could therefore be obtained by this procedure. The diameter of the filament is controllable depending on the die diameter. This implicitly controls the numbers of the nanofibres in the filament as is illustrated in Fig. 4(b). The last step of the nanofibre production is the selective dissolution of PDP in the P4VP/PDP matrix. Fig. 5(a) shows AFM height image of PS nanofibres received through selective dissolution of the matrix and precipitation of the filaments on a silicon substrate. After evaporating the solvent, the PS nanofibres were studied using AFM (tapping mode). Fig. 5(a) shows that the

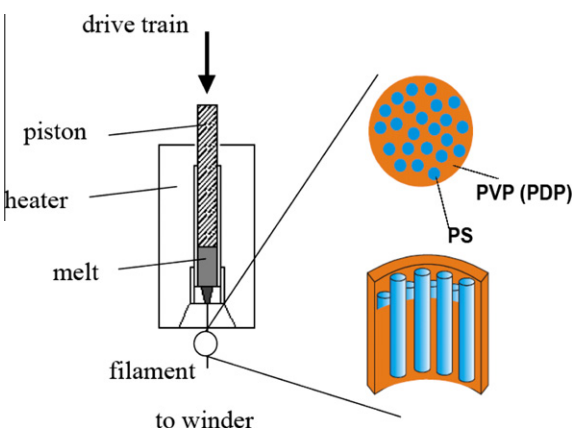

Fig. 3. Schematic drawing of piston type extrusion and spinning device for producing supramolecular assembly nanofibers [37b].

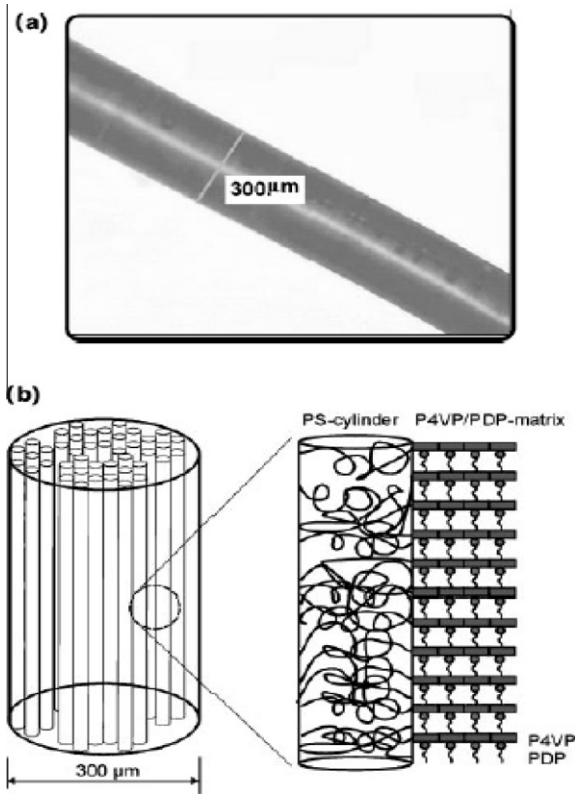

Fig. 4. (a) Light microscopy image from PS-P4VP(PDP)-filament showing a thickness of about 300 μm (b) Structural characteristics of cylinder-within-lamellae structure of PS-block-P4VP(PDP) [38].

nanofibres have lengths on the micron-scale. They can be expected to be even larger before dissolution and precipitation but they may break easily during the dissolution process. This process demonstrates that it is possible to produce anisotropic nanofibres with considerable lengths. The sectional profile in Fig. 5(b) is used to determine the diameter of the nanofibres. Fig. 5(c) shows a 3D-image of the PS nanofibres, presenting smooth PS nanofibres macroscopically oriented with considerable lengths. Due to the low contrast between PS and PVP/PDP matrix in AFM images it was almost impossible to distinguish the phases at very low magnification. By inspecting different adjacent areas, fibres with lengths in the millimetre range have been observed. The diameter of the PS nanofibres was about 110 nm, slightly larger than that observed in the P4VP/PDP matrix. This increase in diameter may be caused by the presence of a P4VP layer around the PS nanofibres due to the presence of chemical connectivity between PS and P4VP (Fig. 5(d)). If the morphology of the supramolecular assemblies is so chosen that the comb block formed the minority component, then porous fibres can also be fabricated. Ikkala and coworkers have shown that by electrospinning, polymeric fibres of PS-*b*-P4VP(PDP) SMA can be prepared in which P4VP(PDP) forms spherical microdomains [39]. The PDP can then be washed to generate porous polymer fibres which potentially could have applications as filters or in functional fabrics.

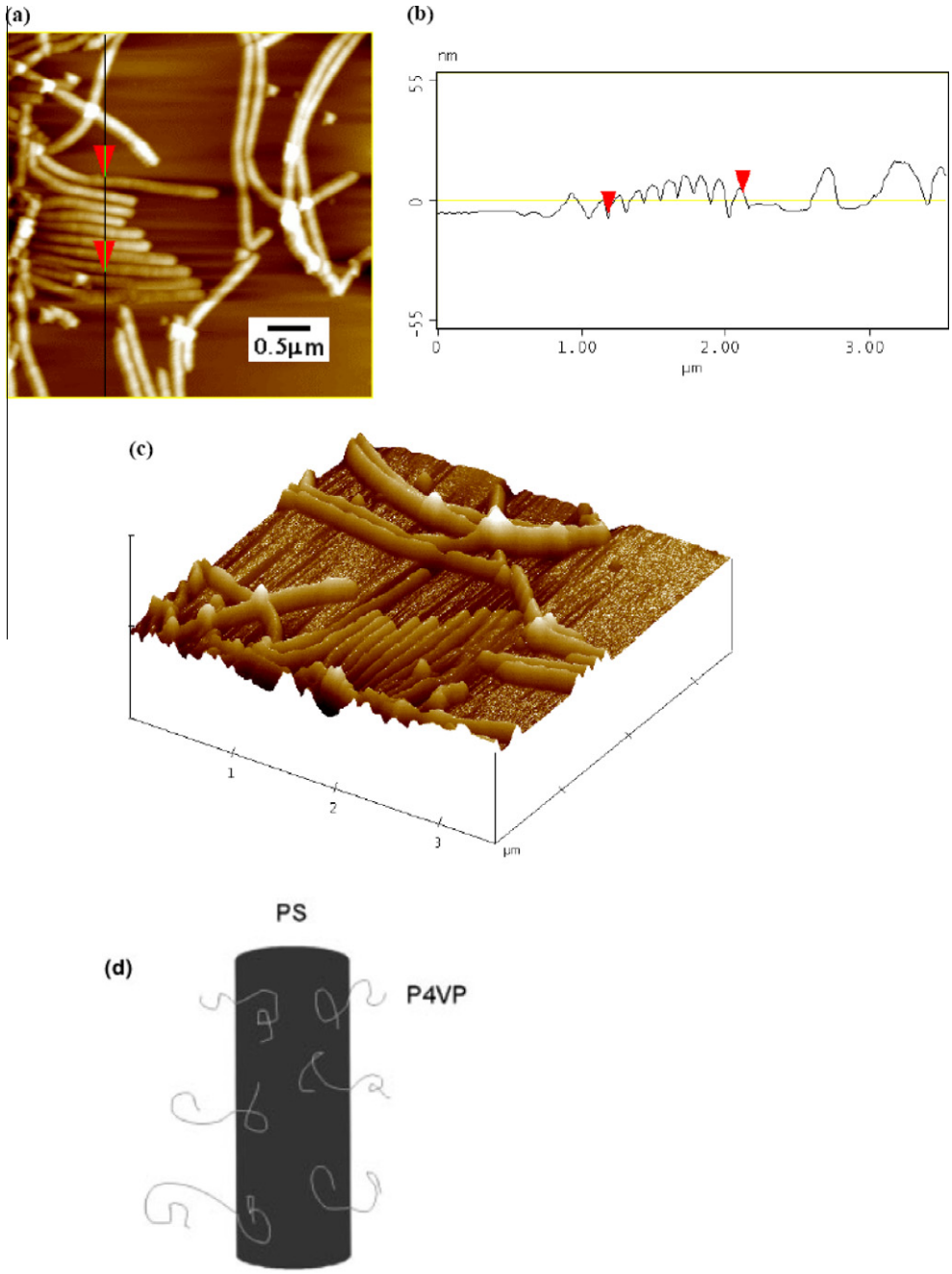

Fig. 5. (a) AFM images of PS nanofibers coated with P4VP layer prepared on Si-substrate (b) sectional profile and (c) 3D-image (d) schematic drawing of PS nanowires with P4VP chains [38].

Using similar procedures, polymeric nanoobjects such as nanosheet and nanospheres can also be produced [40]. For nanosheet fabrication, lamellar morphology of supramolecular assemblies are needed. Fig. 6 shows AFM and TEM images of PS-*b*-P4VP(PDPD) supramolecular assembly with lamellar morphology before and after washing of PDP. The microscopy images before PDP washing showed highly oriented lamellar structure of PS and P4VP(PDP) lamellaes. Washing of PDP leads to the collapse of P4VP chains on PS layer which remains intact producing polymeric nanosheets. The AFM image in Fig. 6 shows such PS nanosheets on a silicon substrate. The sheets lie parallel to each other on the surface with a distance of about (55–60 nm) and an average height of 14 nm. PS nanospheres have been fabricated by Ikkala and co-workers using PS-*b*-P4VP(PDP) SMA with PS spheres embedded in P4VP(PDP) matrix [41].

The thin films of supramolecular assemblies are potentially more attractive as they could allow the fabrication of

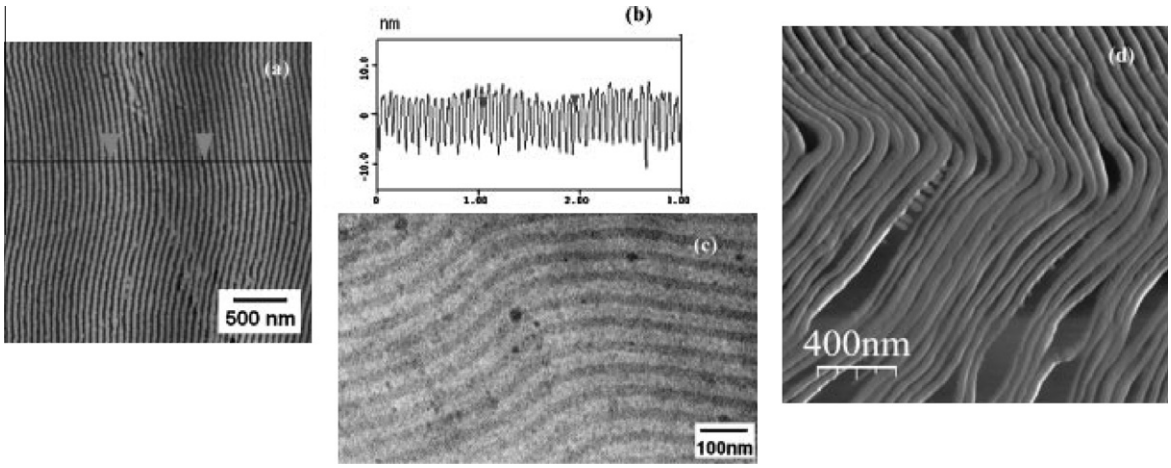

Fig. 6. (a) AFM height image (b) surface profile of the ultrathin section of block copolymer supramolecular assembly on silicon wafer (c) TEM morphology of the ultrathin section (contrast was obtained by staining the P4VP regions with OsO_4) (d) AFM height image of the nanosheet after extraction of PDP [40].

porous nanotemplates. However, the use of surfactants like PDP as low-molecular weight additives in thin films is not feasible since they preferable tend to migrate to the surface of the films and hence the desired morphology could not be obtained. We have shown that, in thin films, the use of additives with functionalities across the molecule might be more useful. In our group, we used HABA as the low-molecular weight additive in thin films of supramolecular assemblies for fabricating porous nanotemplates [17]. Fig. 7 shows a schematic illustration of the process adopted in the present work. The PS-*b*-P4VP was mixed with HABA in a stoichiometric ratio with respect to the 4VP unit in 1,4-dioxane as the solvent medium. HABA, in this case, selectively associates with the pyridine nitrogen of PS-*b*-P4VP via hydrogen bonding and formed SMA (Fig. 7(a)). Thin films of the SMA obtained by dip or spin-coating on a silicon substrate demonstrated vertically oriented hexagonal cylindrical morphology (Fig. 7(c)). The cylindrical nanodomains were formed by the P4VP + HABA complex surrounded by the PS matrix. However, when the SMA was annealed in the vapor of chloroform the cylindrical morphology switched from perpendicular to parallel with respect to the surface plane (Fig. 7(b)). Extraction of HABA with a selective solvent resulted in a porous block copolymer (PBC) film. Depending on the cylinder alignment we obtain PBCs in two forms. The perpendicular cylinder alignment resulted in a nanomembrane, denoted further as PBC⊥, with a hexagonal lattice of hollow channels (Fig. 7(e)). The SMA with the parallel cylinder alignment was turned into PBC|| with a "fingerprint" surface (Fig. 7(d)). Significantly, the walls of the nanochannels or grooves were formed by the reactive P4VP brush. As explained later when the PBC film was dipped into an aqueous solution of pre-synthesized nanoparticles, the solution diffused into the pores driven by capillary force and preferential attraction of the nanoparticle to the P4VP brushes on the wall (Fig. 7(f and g)). The PBC film with the nanoparticles was then UV-cross-linked to stabilize the template. Oxygen-plasma treatment or pyrolysis of the film at 450 °C completely removed the block copolymer film leaving behind nanowire (Fig. 7(i)) or nanodot (Fig. 7(h)) arrays of the nanoparticles on the silicon substrate.

Fig. 8(a–c) show the atomic force microscopy (AFM) topographic images of PS-*b*-P4VP(HABA) SMA films before and after solvent annealing in vapors of different solvents. It must be noted that the AFM images were obtained after washing the SMAs with methanol, which selectively washed out HABA leaving cylindrical cavities in the film. The film directly deposited from 1,4-dioxane and washed with methanol demonstrated pores of 8 ± 1 nm in diameter which were a projection of cylindrical domains with perpendicular orientation, with a periodicity of 24.5 ± 1.5 nm (Fig. 8(a)). The center-to-center distance analysis revealed a relatively narrow distribution of spacing between channels as visualized by the fast Fourier transformation (FFT) image (inset). However, when the SMA films, before methanol washing, were annealed in the vapor of 1,4-dioxane, the long-range order of the cylindrical microdomains increased significantly (Fig. 8(b)). The FFT image showed six sharp first order reflections, which clearly demonstrated that the cylindrical P4VP(HABA) domains were packed in a ordered hexagonal lattice at least over an area of $2 \times 2\ \mu m^2$. Interestingly, when the SMA film solvent casted from 1,4-dioxane solution was annealed in a saturated vapor of chloroform, the cylindrical P4VP(HABA) domains switched to parallel orientation with respect to the surface. Fig. 8(c) shows the AFM image of SMA film, annealed in chloroform and washed with methanol, clearly demonstrating the parallel cylindrical channels with a center-to-center distance of 30 ± 1.5 nm. This re-orientation of the cylinders occurring in SMA is reversible, relatively fast, and can be repeated several times for films that are not rinsed [17].

4. Fabrication of nanomaterials

The templates based on the supramolecular assembly of block copolymer both in bulk and thin film discussed in the

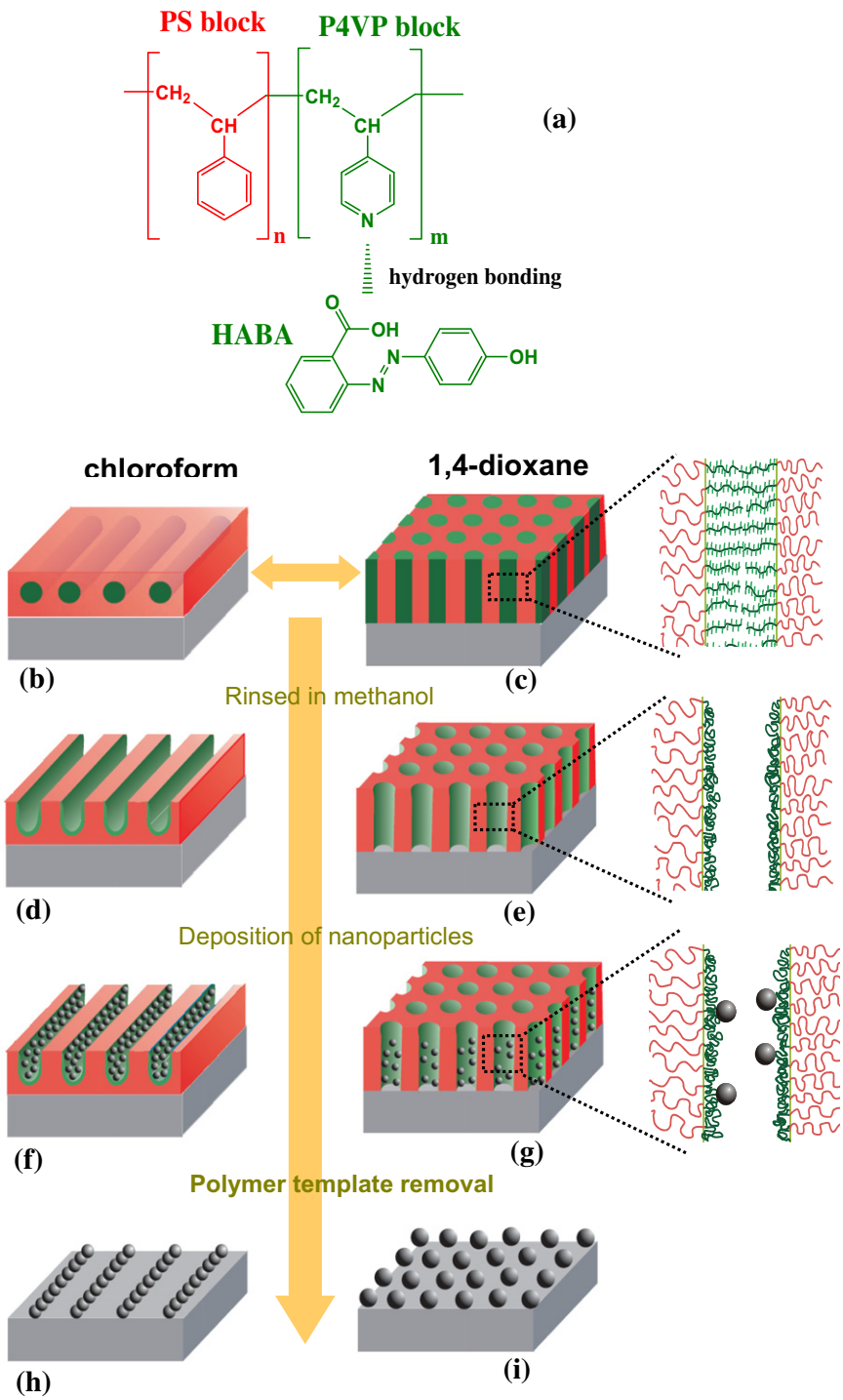

Fig. 7. Schematic illustration of the preparation of block copolymer nanotemplate using supramolecular assembly of PS-*b*-P4VP and HABA for fabrication of inorganic nanodots and nanowire arrays (a) Scheme showing SMA formation through hydrogen bonding between the P4VP block of PS-*b*-P4VP copolymer and HABA. Thin film of PS-*b*-P4VP(HABA) SMA annealed in (b) chloroform and (c) 1,4-dioxane. (d and e) Rinsing the SMA thin films in methanol washes away HABA leaving cylindrical channels/pores, in the PS matrix, whose walls are lined with collapsed P4VP chains. (f and g) After dipping the SMA nanotemplates into aqueous solution of nanoparticles. (h and i) The polymer is removed by oxygen plasma etching or by pyrolysis at 450 °C leaving inorganic nanowires and nanodots on the substrate surface [49].

last section were further used for a variety of nanofabrication processes. The nanofibers produced using supramolecular assembly between PS-*b*-P4VP and PDP after applying shear flow can be further used to fabricate metallic and

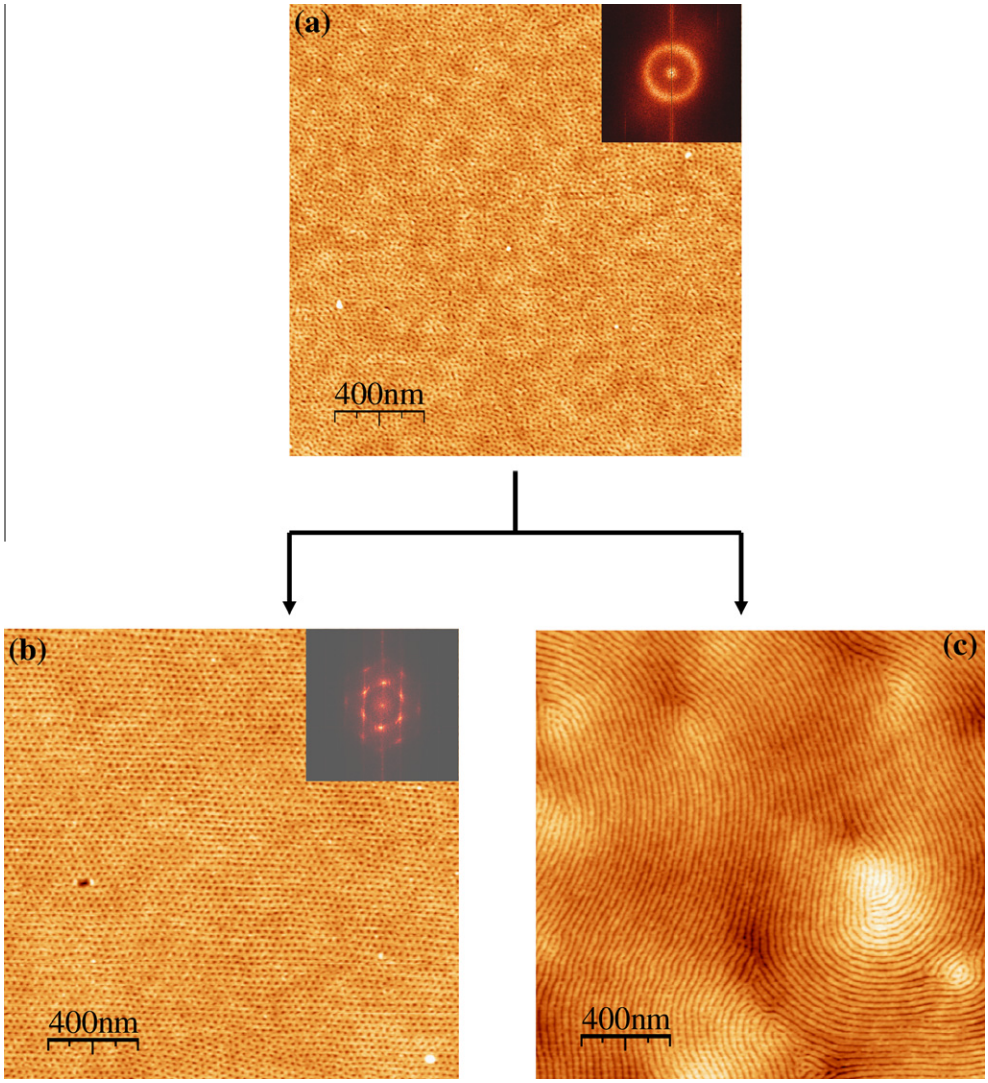

Fig. 8. AFM height images of the SMA thin film obtained after HABA extraction. (a) Dip-coated SMA films from 1,4-dioxane solution. (b) After annealing in 1,4-dioxane vapor. (c) After annealing in chloroform vapor [49].

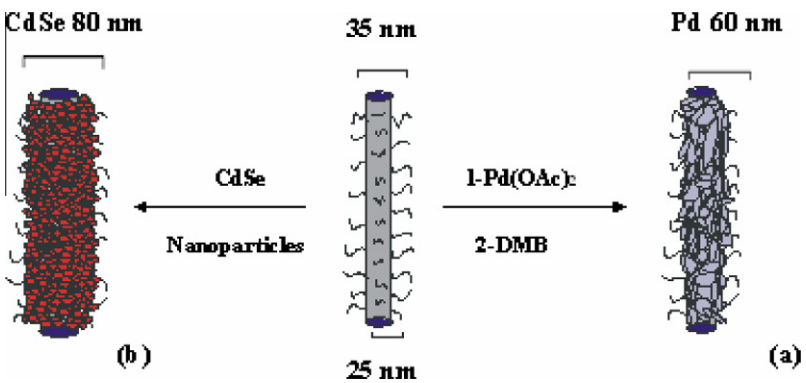

Fig. 9. Schematic diagram of the metallization route starting from the polymeric nanofibers fabricated using supramolecular assembly between PS-*b*-P4VP and PDP (a) reduction and complexation of Pd ions with P4VP on Si-substrate. (b) Adsorption of CdSe nanoparticles on P4VP [37a].

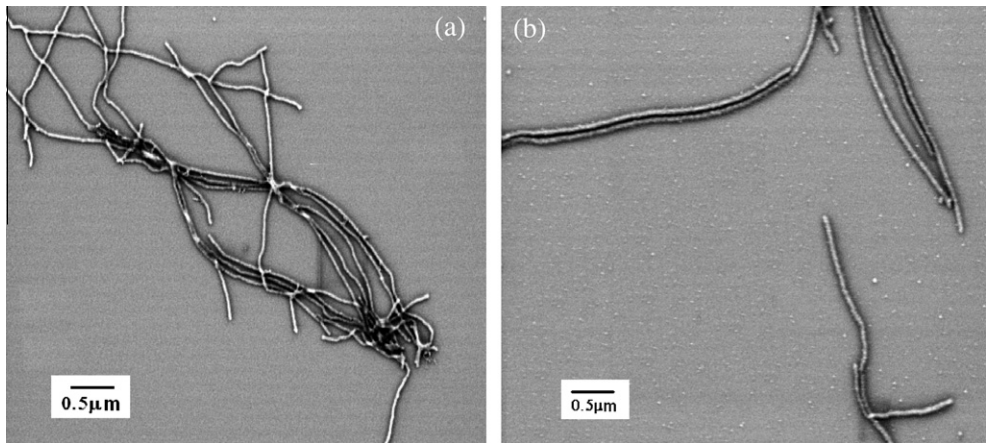

Fig. 10. SEM image of (a) Pd nanowires (diameter of 60 nm) and (b) CdSe nanowires (90 nm) fabricated from block copolymer supramolecular assembly [37a].

semiconducting nanowires [37a] of several μm length according to the scheme depicted in Fig. 9. For example Metallic Pd nanowires with diameter of 60 nm and several μm in length have been successfully synthesized by reduction of $Pd(CH_3COO)_2$ deposited on block copolymer nanofiber surface with $(CH_3)_2NBH_2$ (Fig. 10(a)). Similarly semiconductor nanowires of CdSe are fabricated by adsorption of CdSe nanoparticles (size approx. 2 nm) onto 35 nm nanofibers to produce nanowires of 80 nm in width (Fig. 10(b)). Ikkala et al. [41,42] fabricated hollow inorganic nanotubes and nanospheres of different material like clay, alumina using block copolymer template from supramolecular assembly as scaffold material.

Ultrathin microtomed films of 40–50 nm prepared from bulk sample and oriented under large amplitude oscillatory shear (LAOS) can also be further used for nanofabrication. Fig. 11 depicts the decoration of the ultrathin microtomed film with Pd metal nanoparticles which selectively deposited on one of the block copolymer microdomain. This decoration of the block copolymer ultrathin film resulted in the nano-scale alignment of metal nanocluster with a narrow size distribution within block

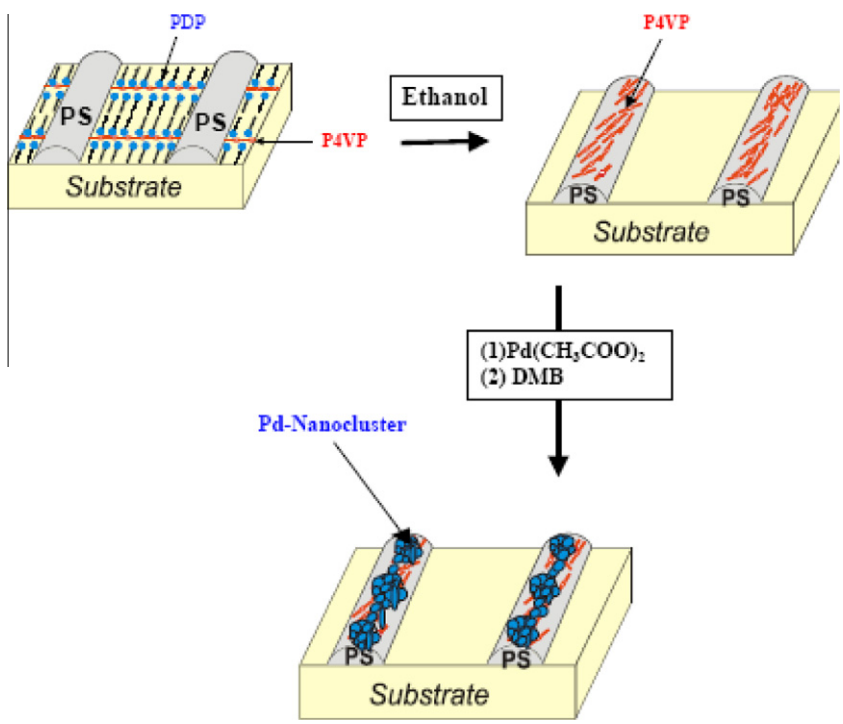

Fig. 11. Schematic diagram for the decoration of the ultrathin microtomed block copolymer supramolecular thin film with Pd nanoparticle [37b].

copolymer ultrathin films. Fig. 12 shows the AFM height image of the ultra thin microtomed block copolymer thin film with its section analysis. Sectional analysis of AFM measurements shows phase segregated nanodomains ranging in size from 120 to 140 nm in width, with an aspect of height approximately 30 nm. From the AFM image it can be concluded that the nanosheets microdomains are maintained during the reduction and solvent evaporation process where as the Pd(II) incorporated in the P4VP phase does not perturb the sheets microdomains structure.

Thin films fabricated using supramolecular assembly of PS-*b*-P4VP and HABA discussed earlier have been used for variety of different nanofabrication. High density arrays of ordered and aligned polyaniline nanorods with 10 nm diameter have been successfully fabricated on transparent ITO substrate via electropolymerization (Fig. 13). The ordered arrays of polyaniline nanorods (Fig. 14(a and b)) fabricated in this way exhibit excellent electrochemical properties with an electrochemical capacitance value of 3407 Fg^{-1} [11]. Recently, ten Brinke et al. [43] reported the chemical synthesis of polypyrrole nanostructured thin film from PS-*b*-P4VP(PDP) supramolecular assembly.

Also in an electrochemical process, Nickel was introduced into the perpendicular cylindrical channels of the SMA nanotemplate in galvanostatic mode or by pulse plating [17a]. Fig. 15 depicts an AFM height image of the nickel dots, corresponding Power Spectral Density and Fast Fourier Transformation of the structure after the polymer template has been removed. However, keeping the polymer film on the substrate after deposition has additional benefits in this example. Investigation of the oxidation state of the nickel rods with X-ray absorption spectroscopy

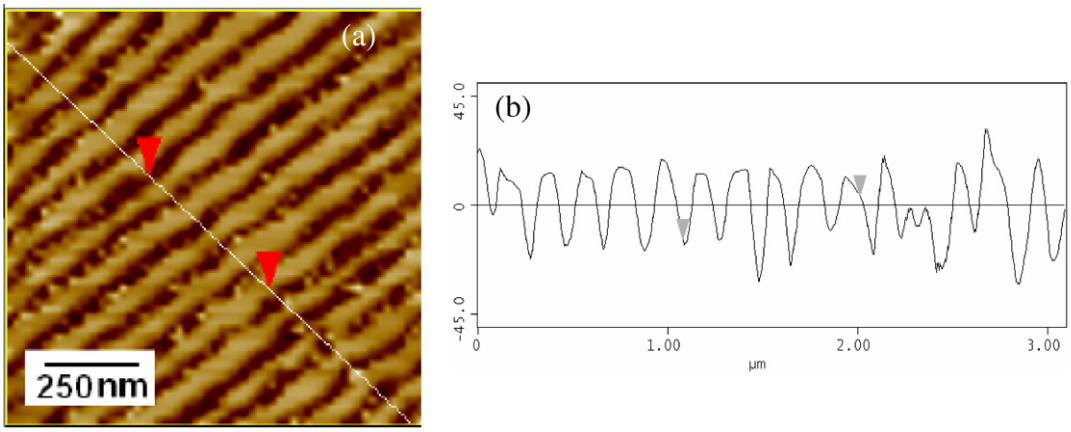

Fig. 12. (a) AFM phase image shows diffusion of Pd ions into P4VP phase (b) section profile along the line.

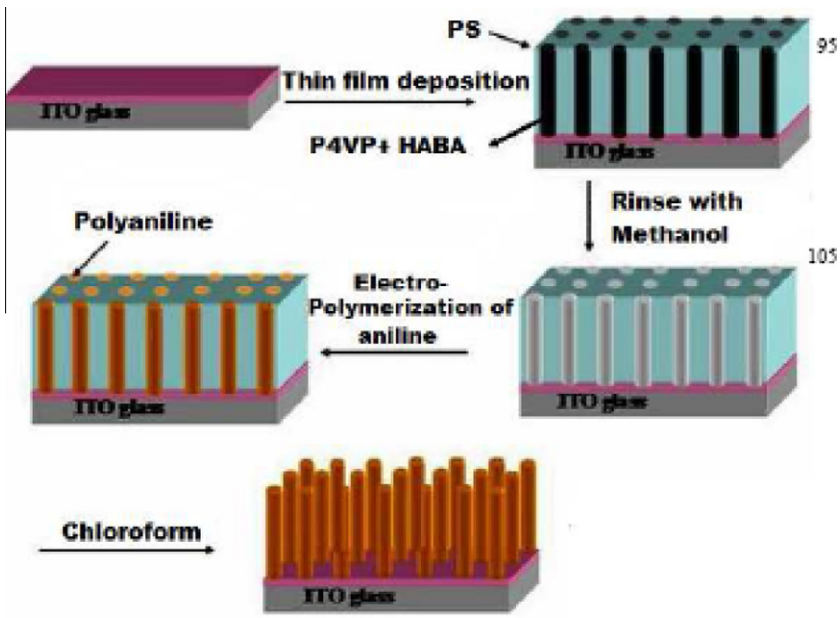

Fig. 13. Schematic presentation for fabrication of polyaniline nanorods using block copolymer nonporous template [11].

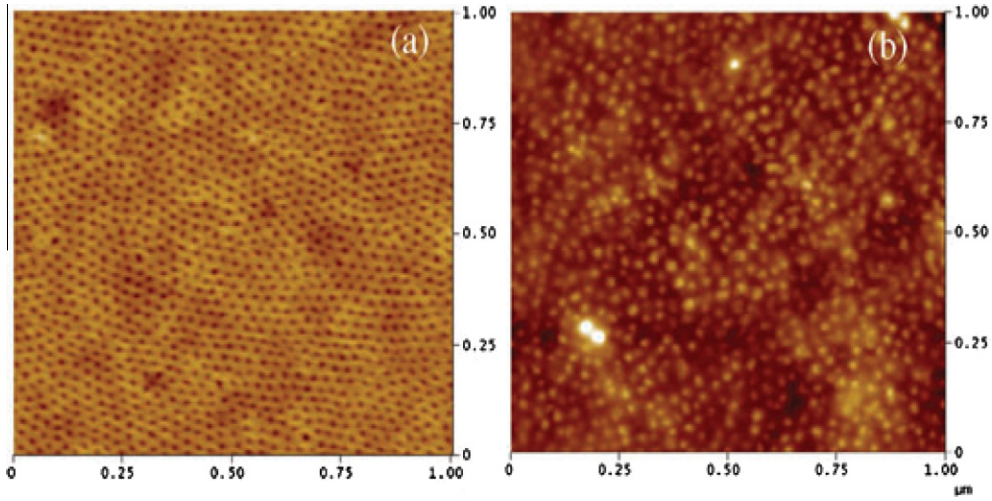

Fig. 14. AFM height images of (a) block copolymer nanotemplate (b) polyaniline nanorods. The total scale bar is 1 μm [11].

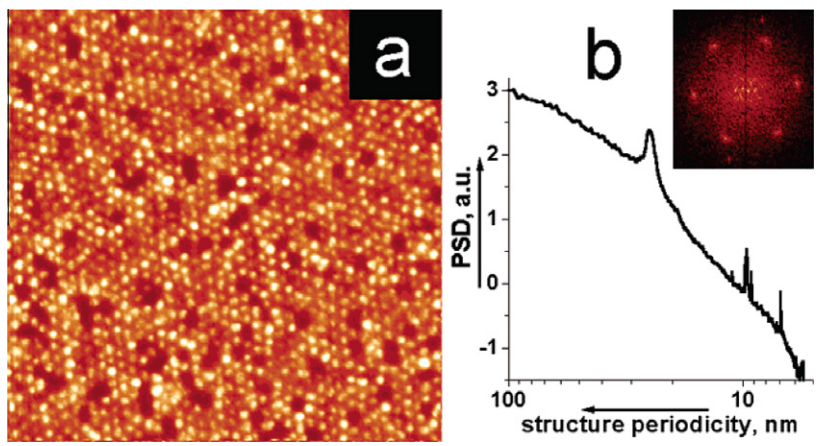

Fig. 15. Ni dots electrodeposited throughout 45 nm thick PS-PVP nanotemplate, lateral scale 1 × 1 μm^2: (a) topography image, *z* scale 30 nm, (b) power spectrum density, the main peak (24 nm) corresponds to the SMA periodicity (inset, FFT image of (a) showing perfect hexagonal ordering of Ni dots). Occasional lacunas appear due to the inhomogeneity of electrodeposition [17a].

and X-ray photoelectron spectroscopy at the Ni L edges give evidence that the Ni rods were metallic despite their preparation under ambient conditions as no hints for NiO complexes were found inside the particles. This indicates that the remaining polymer film protects Ni nanoparticles against oxidation [44].

The SMA templates could also be used for patterning polymeric materials which cannot be electropolymerized. Under the direction of interpolymer hydrogen bonding and capillary action of nanopores, SMA templates were properly filled with phenolic resin precursor, followed by curing and pyrolysis at middle temperature to remove the nanotemplate. As a result, polymer nanodot arrays (see Fig. 16) were obtained with spacing below 30 nm [45].

When additional process steps are added, new structures can be obtained from the templates. For example silica nanodots, which were prepared by pyrolysis of a SMA template loaded with a precursor species, were used to guide the dewetting of a phenolic resin precursor thin film. Curing and calcination of the phenolic precursor, followed by etching of the silica arrays, results in large area carbon nanoring arrays (Fig. 17) with a diameter as small as 25 nm [46]. Ikkala et al. [47] reported the fabrication of porous functional material with a narrow distribution of pore sizes, high density of pores, large surface area per volume unit, and selective absorption properties using templates of block copolymer and phenolic resin.

Optically active SMA nanotemplates were also developed. For this, two different techniques are used for functionalization of PS-*b*-P4VP based nanotemplates [48]. Either a luminescent additive (e.g. 1-pyrenemethanol – PyM) is incorporated into the SMA instead of HABA (direct funtionalization). Compared to a thin film consisting of PyM and carboxy-terminated polystyrene, the PS-*b*-P4VP(PyM) complex shows greatly reduced eximer emission in the PL spectra (Fig. 18). For the second approach,

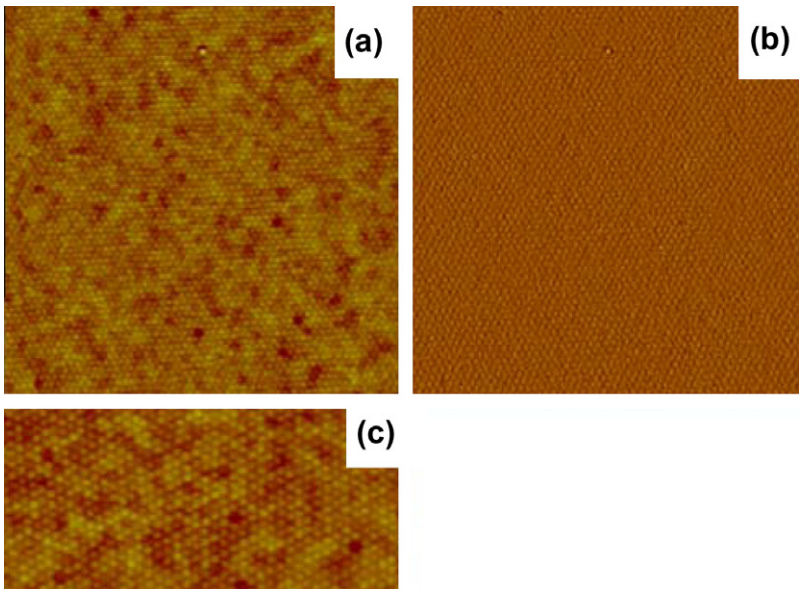

Fig. 16. AFM images of highly ordered polymeric nanodots arrays from nanoporous thin film after pyrolysis. (a) height image, (b) phase image. Lateral scale 1500 × 1500 nm. (c) Enlarged height image [45].

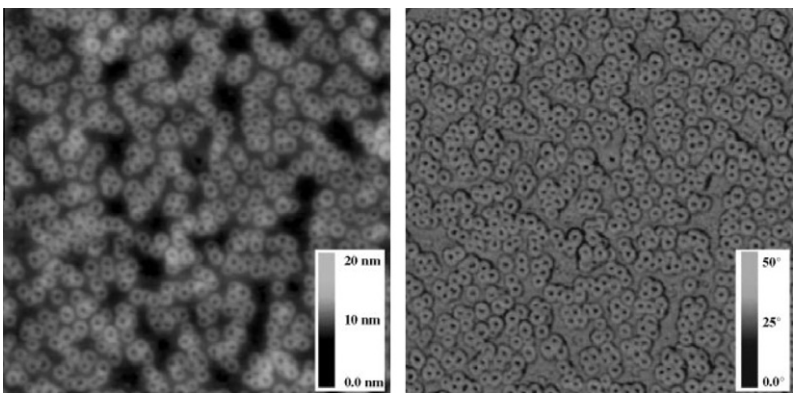

Fig. 17. AFM images of carbon nanoring arrays on a silicon wafer after removing the silicate nanodot template. Left: height image. Right: phase image; lateral scale 1 × 1 μm [46].

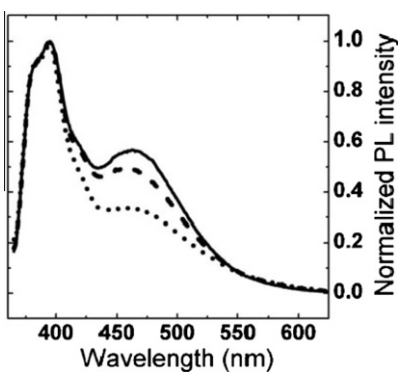

Fig. 18. Normalized photoluminescent emission of 30-nm films made of: PyMþPSCOOH (solid), PS-*b*-P4VP(PyM) (from toluene) without annealing (dash) and after annealing (dot). Excitation wavelength was 345 nm [48].

so called post-functionalization, washed and UV-cross-linked nanotemplates developed from PS-*b*-P4VP(HABA) are impregnated with a dilute solution of a dye (rhodamine 6G) in methanol or 1,4-dioxane. Absorption and PL spectra shown in Fig. 19 give evidence, that the optical properties in post-functionalization are rather governed by solvent and agglomeration effects than by the properties of the template.

Similar to the post-functionalization of the nanotemplate with dye molecules, several other materials can be incorporated into the porous structure of the washed SMA templates. A simple route to fabricate highly dense arrays of palladium nanodots and nanowires with sub-30 nm periodicity was presented by the direct deposition of pre-manufactured palladium nanoparticles from aqueous solution. The metal particles selectively migrate in

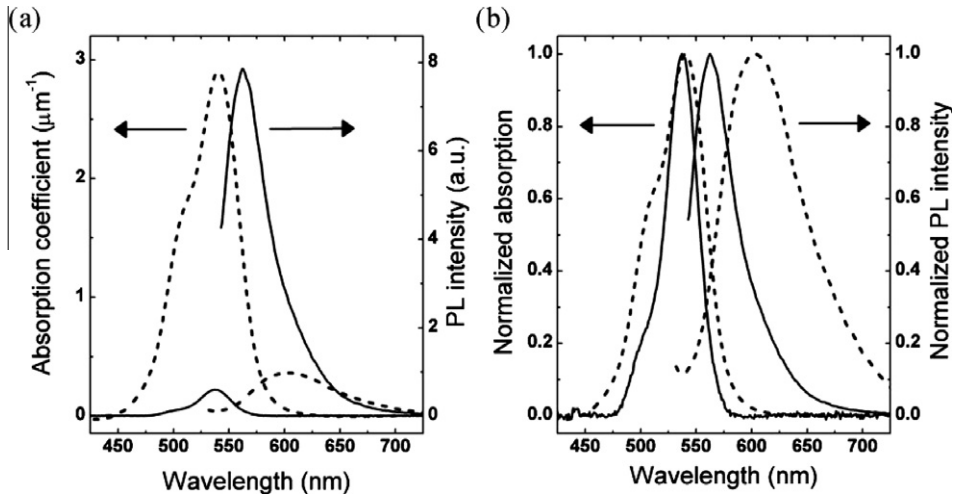

Fig. 19. (a) UV–vis absorption and PL emission, and (b) normalized spectra of 50-nm films prepared via soaking of porous crosslinked nanotemplates in 1,4-dioxane (dash) and methanol (solid) solutions of R6G [48].

the pores mainly due to their preferential attraction to the P4VP block covering the pore wall. The polymer template was then removed by oxygen plasma etching or pyrolysis in air resulting in palladium nanostructures whose large scale morphology mirror that of the original template (Fig. 20). The method adopted is general and versatile so that it could be easily extended for patterning a variety of metallic materials into dot and wire arrays [49].

Comparable to classic lithography, developed SMA template structures can be transferred into the underlying substrate by Reactive Ion Etching [50]. Fig. 21 shows cross-sectional transmission electron micrograph of a

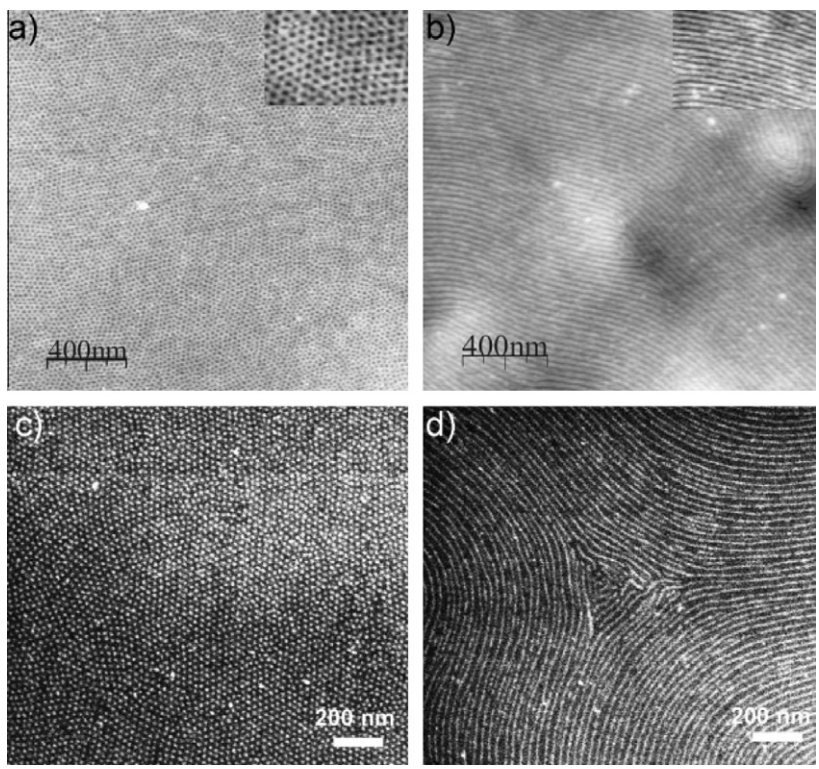

Fig. 20. Nanotemplates after the deposition of palladium nanoparticles from solution. (a and c) AFM height and HRSEM images, respectively, of template with perpendicular orientation. (b and d) AFM height and SEM image, respectively, of the parallel oriented sample. The palladium nanoparticles were not observed in the AFM images since they were present inside the pores/channels [49].

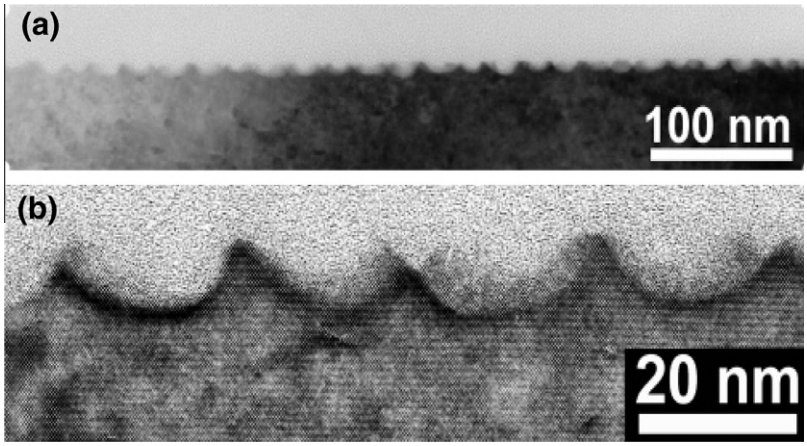

Fig. 21. TEM micrographs of cross-sectional specimens of patterned Si wafers: (a) over-view; (b) details [50].

silicon wafer, which was homogeneously patterned over large areas, as obvious from Fig. 21(a). The period of about 26 nm is in line with that of the used SMA template. A detailed view (Fig. 21(b)) reveals that the indentations have a depth of about 10 nm. No amorphous silica layer covering the Si is present. The low aspect ratio of the produced structures can be attributed to the nearly complete consumption of the polymer template during the etch step.

One possible method to reinforce the polymer against etching is to convert the polymer into a carbonized nanostructured thin films involving ion beam treatment. During this process, the film thickness is reduced by approximately 50%, but it retains hexagonal nanomorphology [51]. The films are mechanically robust, stable at high temperatures and well suited for applications as ultrafiltration membranes, quantum dot or single molecule supports, masks for nanolithography. By superimposing two carbonized thin films, rotation moiré patterns are observed (Fig. 22) [52]. Periodic hexagonal moiré superstructures appear when the films possessing long-range order are superimposed at small misorientation angles while overlapping films misoriented by angles close to 30° generate aperiodic quasi-crystal-like superstructures with 5-fold symmetries [52]. Especially the latter are interesting, as quasi-crystal structures at this length scale cannot be obtained by other methods.

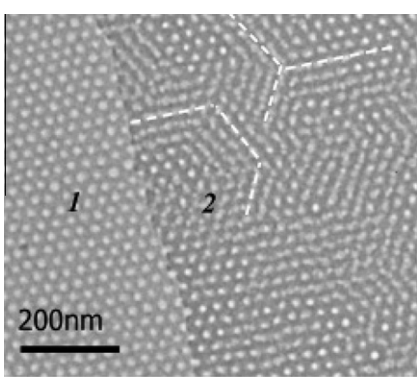

Fig. 22. TEM image of stacked carbonized nanotemplate films showing the boundary of one of the single- and the double-layer zones. A few moiré fringes are designated with a dashed white line for eye-guiding; numbers indicate the number of the layers in the corresponding zones [51].

5. Summary and outlook

The work done over last few years on block copolymer SMAs have shown tremendous potential of these materials in nanofabrication. Moreover, investigation on the fundamental aspects of microphase separation in these SMAs has further added to the already existing knowledge about the complex nature of block copolymer self-assembly in thin films. However, block copolymer SMAs are still an emerging area of research and recently several other research groups have started focusing on block copolymer SMAs. However, a number of fundamental and technological aspects of block copolymer SMAs still have to be solved.

The cylindrical microdomains in the SMA were shown to switch their orientation depending on the annealing solvent and a plausible mechanism was also discussed. A better understanding of the switching mechanism should be still obtained using in situ GISAXS during exposure of the SMA thin films to solvent vapors. Such studies are expected to clearly resolve the pathway for the switching of cylinder orientation by providing information about the transient structures. The long-range order of the structures is very important especially for the nano-patterned structures to be ultimately incorporated in functional devices and several groups are currently working towards developing methods for increasing the long-range order in these SMAs. Our work so far has mostly involved HABA as the low-molecular weight additive, but a number of other low molecular additive should be available in order to synthesize SMAs with a range of different properties. The recent work of Mezzenga and co-workers [53] and Xu and co-workers [54,55] where they incorporated semiconducting low-molecular weight additive/nanoparticles in the block copolymers demonstrates the future potential of the SMA approach. Furthermore, we have shown that the SMA templates could be extremely useful for fabricating conducting

polymer and magnetic nanorods by electrochemical methods. Further work needs to be done for fabrication of such materials with a focus on optimization of the fabrication procedures, tuning of size, spacing and aspect ratio of the nanostructures, extending the approach to fabricate variety of conducting and magnetic nanomaterials, and property evaluation of such materials. The porous nanotemplates obtained from SMAs are also expected to be excellent candidates for use in membrane application. Supramolecular assemblies of block copolymers are thus still challenging systems with promising perspectives for fabrication of nanomaterials taking also the fascinating advances of block copolymer chemistry into account.

Acknowledgements

This research was supported by the priority program of Deutsche Forschungsgemeinschaft (SPP1165). The authors thank Prof. Alexander Sidorenko, Dr. Igor Tokarev, Prof. Sergiy Minko, Dr. Radim Krenek, Dr. E. Bhoje Gowd, Dr. Valeriy Luchnikov, Dr. Frank Böhme, Dr. Petr Formanek, Dr. Xikiu Liu, Dr. Petr Formanek, Dr. Amir W. Fahmi, Prof. N. Zafeiropoulos, Mr. A. Janke, Mr. Marcus Böhme and Mr. Y. Sun for their contributions in the work discussed here. The authors also thank Dr. Martin Steinhart, Dr. Sebastian Fähler, Dr. O. Seifarth, Dr. D. Schmeißer and Prof. Alexander Eychmüller with whom they collaborated during the course of this work. One of the authors (B.K.) acknowledges financial support from the Alexander von Humboldt foundation.

References

[1] Landis S, Rodmacq B, Dieny B. Phys Rev B 2000;62:12271.
[2] Chou SY. Proc IEEE 1997;85:652.
[3] Rettner CT, Anders S, Thomson T, Albrecht M, Best ME, Terris BD. IEEE Trans Magn 2002;38:1725.
[4] (a) Bates FS, Fredrickson GH. Annu Rev Phys Chem 1990;41:525–57; (b) Hadjichristidis N, Pitsikalis M, Iatrou H. Adv Polym Sci 2005;189:1–124; (c) Hadjichristidis N, Pispas S, Floudas GA. In: Block copolymers. Synthetic strategies, physical properties, and applications. Weinheim: Wiley; 2003.
[5] (a) Park S, Wang JY, Kim B, Xu J, Russell TP. ACS Nano 2008;2:766; (b) Park S, Wang JY, Kim B, Russell TP. Nano Lett 2008;8:1667; (c) Misner MJ, Skaff H, Emrick T, Russell TP. Adv Mater 2003;15:221; (d) Zhang Q, Xu T, Butterfield D, Misner MJ, Ryu DY, Emrick T, et al. Nano Lett. 2005;5:357.
[6] Mansky P, Chaikin PM, Thomas EL. J Mater Sci 1995;30:1987.
[7] Haberkorn N, Lechmann MC, Sohn BH, Char K, Gutmann JS, Theato P, et al. Macromol Rapid Commun 2009;30:1146.
[8] Park M, Harrison C, Chaikin PM, Register RA, Adamson DH. Science 1997;276:1401.
[9] Lo K-H, Chen M-C, Ho R-M, Sung H-W. ACS Nano 2009;3:2660.
[10] Rider DA, Liu K, Eloi J-C, Vanderark L, Yang L, Wang J-Y, et al. ACS Nano 2008;2:263.
[11] Kuila BK, Nandan B, Böhme M, Janke A, Stamm M. Chem Comm 2009:5749.
[12] Lee JI, Cho SH, Park S-M, Kim JK, Kim JK, Yu J-W, et al. Nano Lett 2008;8:2315.
[13] Valkama S, Ruotsalainen T, Nykanen A, Laiho A, Kosonen H, ten Brinke G, et al. Macromolecules 2006;39:9327.
[14] Ruokolainen J, Saariaho M, Ikkala O, ten Brinke G, Thomas EL, Torkkeli M, et al. Macromolecules 1999;32:1152.
[15] Ikkala O, ten Brinke G. Chem Commun 2004;6:2131.
[16] Osuji CO, Chao CY, Ober CK, Thomas EL. Macromolecules 2006;39:3114.
[17] (a) Sidorenko A, Tokarev I, Minko S, Stamm M. J Am Chem Soc 2003;125:12211(b) Tokarev I. Ph.D. Dissertation. Technische Universität Dresden; 2005.
[18] van Zoelen W, Asumaa T, Ruokolainen J, Ikkala O, ten Brinke G. Macromolecules 2008;41:3199.
[19] (a) Tokarev I, Krenek R, Burkov Y, Schmeisser D, Sidorenko A, Minko S, et al. Macromolecules 2005;38:507(b) Krenek R, Ph.D. Dissertation. Technische Universität Dresden, 2008.
[20] Laforgue A, Bazuin CG, Prudhomme RE. Macromolecules 2006;39:6473.
[21] Tung S-H, Kalarickal NC, Mays JW, Xu T. Macromolecules 2008;41:6453.
[22] (a) Kosonen H, Ruokolainen J, Knaapila M, Torkkeli M, Serimaa R, Bras W, et al. Synth Met 2001;121:1277; (b) van Ekenstein GA, Polushkin E, Nijland H, Ikkala O, ten Brinke G. Macromolecules 2003;36:3684.
[23] Wood KC, Little SR, Langer R, Hammond PT. Angew Chem Int Ed 2005;44:6704.
[24] Faul CFJ, Antonietti M. Adv Mater 2003;15:673.
[25] Thunemann AF. Prog Polym Sci 2002;27:1473.
[26] Valkama S, Lehtonen O, Lappalainen K, Kosenen H, Castro P, et al. Macromol Rapid Commun 2003;24:556.
[27] Ruokolainen J, Tanner J, ten Brinke G, Ikkala O, Torkelli M, Serimaa R. Macromolecules 1995;28:7779.
[28] Morikawa Y, Nagano S, Watanabe K, Kamata K, Iyoda T, Seki T. Adv Mater 2006;18:883.
[29] Chao CY, Li XF, Ober CK, Osuji C, Thomas EL. Adv Funct Mater 2004;14:364.
[30] Ruokolainen J, Makinen R, Torkkeli M, Makela T, Serimaa R, ten Brike G, et al. Science 1998;280:557.
[31] Ikkala O, ten Brinke G. Science 2002;295:2407.
[32] Kosonen H, Valkama S, Ruokolainen J, Torkkeli M, Serimaa R, ten Brine G, et al. Eur Phys J 2003;10:69–75.
[33] Mäki-Ontto R, de Moel K, Polushkin E, Alberda van Ekenstein G, ten Brinke G, Ikkala O. Adv. Mater. 2002;14:357–61.
[34] Ruotsalainen T, Torkkeli M, Serimaa R, Mäkelä T, Mäki-Ontto R, Ruokolainen J, et al. Macromolecules 2003;36:9437–42.
[35] Nandan B, Vyas MK, Böhme M, Stamm M. Macromolecules 2010;43:2463–73.
[36] (a) Chen HL, Lu JS, Yu CH, Yeh CL, Jeng US, Chen WC. Macromolecules 2007;40:3271–6; (b) Chiang W-S, Lin C-H, Yeh C-L, Nandan B, Hsu P-N, Lin C-W, et al. Macromolecules 2009;42:2304–8.
[37] (a) Fahmi AW, Braun H-G, Stamm M. Adv Mater 2003;15:1201 (b) Fahmi AW. Ph.D. Dissertation. Technische Univerität Dresden: 2003.
[38] Fahmi AW, Brünig H, Weidisch R, Stamm M. Macromol Mater Eng 2005;290:136.
[39] Ruosalainen T, Turku J, Heikkilä P, Ruokolainen J, Nykänen A, Laitinen T, et al. Adv Mat 2005;17:1048.
[40] Fahmi AW, Gutmann JS, Roland V, Gindy N, Stamm M. Macromol Mater Eng 2006;291:1061.
[41] Ras RHA, Ruotsalainen T, Laurikainen K, Linder MB, Ikkala O. Chem Commun 2007:1366–8.
[42] Ras HA, Kemell M, de Wit J, Ritala M, ten Brinke G, Leskelä M, et al. Adv. Mater 2007;19:102–6.
[43] van Zoelen W, Bondzic S, Landaluce TF, Brondijk J, Loos K, Schouten A-J, et al. Polymer 2009;50:3617–25.
[44] Seifarth O, Krenek R, Tokarev I, Burkov Y, Sidorenko A, Minko S, et al. Thin Solid Films 2007;515:6552.
[45] Liu X, Stamm M. Nanoscale Res Lett 2009;4:459.
[46] Liu X, Stamm M. Macromol Rapid Comm 2009;30:1345.
[47] Kosonen H, Valkama S, Nykänen A, Toivanen M, ten Brinke G, Ruokolainen J, et al. Adv Mater 2006;18:201–5.
[48] Krenek R, Cimrová V, Stamm M. Macromol Symp 2008;268:86.
[49] Nandan B, Gowd EB, Bigall NC, Eychmüller A, Formanek P, Simon P, et al. Adv Func Mater 2009;19:2805.
[50] Zschech D, Milenin AP, Scholz R, Hillebrand R, Sun Y, Uhlmann P, et al. Macromolecules 2007;40:7752.
[51] Kondyurin A, Bilek M, Janke A, Stamm M, Luchnikov V. Plasma Processes Polym 2008;5:155–60.
[52] Luchnikov V, Kondyurin A, Formanek P, Lichte H, Stamm M. Nano Lett 2007;7:3628.
[53] Sary N, Richard F, Brochon C, Leclerc N, Leveque P, Audinot JN, et al. Adv Mater 2010;22:763.
[54] Rancatore BJ, Mauldin CE, Tung S-H, Wang C, Hexemer A, Strzalka J, et al. ACS Nano 2010;4:2721.
[55] Zhao Y, Thorkelsson K, Mastroianni AJ, Schilling T, Luther JM, Rancatore BJ, et al. Nat Mater 2009;8:979

Dr. Bhanu Nandan (born 1974) studied polymer science at the G J University of Science and Technology, India. Subsequently he worked as a research fellow at the Defence Research & Development Organization India in its Kanpur laboratory and obtained his doctorate in Applied Chemistry (Polymer Science) from Kanpur University in 2003. After completion of his PhD, he joined as a postdoctoral researcher in the research group of Prof. Hsin-Lung Chen at the Department of Chemical Engineering, National Tsing Hua University, Taiwan. In 2006, he joined Prof. Manfred Stamm's research group, at Leibniz Institute of Polymer Research Dresden, Germany as a Guest Scientist. Since June 2010 he is an Assistant Professor at the Department of Textile Technology, Indian Institute of Technology Delhi, India. His current research focuses on novel routes for fabricating nanostructured polymer fibres, block copolymer based nanotechnology, and scattering techniques in polymer.

Dr. Biplab K Kuila (born 1978) studied physical chemistry at the University of Calcutta, India and obtained his doctorate in polymer Science from the Jadavpur University, India. After completion of his PhD, he joined as postdoctoral Researcher in the research group of Prof. Liming Dai, Department of Chemical and Materials Engineering, University of Dayton, USA. In 2009, he joined Prof. Manfred Stamm's research group at Leibniz Institute of Polymer Research Dresden, Germany as Alexander von Humboldt Fellow. His current research focuses on block copolymer supramolecular assembly and nanofabrication.

Prof. Dr. Manfred Stamm (born 1949) studied physics at University of Frankfurt am Main and at Bristol University in England for one year. In 1974 he obtained his diploma in solid state physics. In 1979 he finished his PhD at the Institute of Physical Chemistry of University of Mainz with Prof. Dr. E. W. Fischer (neutron scattering and magnetooptic measurements). During this time he continued at CNRS/ Max-Planck Institute of Solid State Physics in Grenoble, France for three years. From 1979 - 1985 Prof. Dr. Stamm was the staff scientist at Institute of Solid State Research at Research Center Jülich and in 1984 became a visiting scientist to Brookhaven National Laboratory/ United States. He then joined the Max-Planck Institute of Polymer Research in Mainz as a staff scientist and project leader and subsequently received his professorship at Dresden in 1999. He now is professor for Physical Chemistry of Polymeric Materials at the Technical University Dresden and head of IPF-Institute of Physical Chemistry and Physics of Polymers at Leibniz Institute of Polymer Research Dresden, Germany. His main activities are in nanostructured materials, polymer surfaces and interfaces, mechanical properties and biocompatible materials.